

The air kerma-rate constant of high dose-rate Ir-192 sources

Matthew B. Podgorsak,¹ Larry A. DeWerd, and Bhudatt R. Paliwal

Departments of Medical Physics and Human Oncology, University of Wisconsin, Madison, Wisconsin, 53792. ¹Present address: Department of Radiation Medicine, Roswell Park Cancer Institute Buffalo, New York 14263

The current value of the air kerma rate constant used in dosimetry calculations for high dose-rate (HDR) Ir-192 sources is based on photon spectral information obtained with low activity Ir-192 sources different in size and encapsulation from the HDR Ir-192 sources used today. Since source configuration has been shown to affect the photon spectrum emitted by a radionuclide, the purpose of this work is to measure the photon spectrum emitted by an HDR Ir-192 source. To simplify the spectral measurements and increase the accuracy of the resulting spectrum, an Ir-192 source identical dimensionally to a clinical source but activated to as low an activity as technically possible was obtained from the manufacturer. Spectral measurements were made with a high purity germanium detector interfaced to a multichannel analyzer. It was found that the HDR source capsule attenuates photons with energies below 500 keV. In fact, no photons with energy below 60 keV can be identified in the HDR Ir-192 photon spectrum, even though the decay of Ir-192 results in several characteristic x-rays in this energy range. As a result, the fluence-weighted and energy-fluence-weighted average energies of the HDR Ir-192 spectrum were found to be 371 and 402 keV, respectively, higher than the average energies of a bare Ir-192 source. A calculation of the HDR Ir-192 air kerma-rate constant based on the measured photon spectrum gives a value of $(29.02 \pm 0.26) \times 10^{-18} \text{ Gy m}^2 \text{ Bq}^{-1} \text{ s}^{-1}$, $\sim 5\%$ lower than the value currently associated with HDR Ir-192 sources. The serious potential clinical implications resulting from this discrepancy in air kerma rate constant strongly support the abolishment of source activity in favor of reference air kerma rate for HDR Ir-192 source strength specification.

Key words: brachytherapy; iridium radioisotopes; radiotherapy dosage; spectrum analysis; photons

Introduction

Presently, the most commonly used high dose-rate (HDR) remote afterloader in North America is the Microselectron (Nucletron Corpora-

tion, Leersum, Holland). This unit houses a single iridium (Ir-192) source with a nominal activity of 370 GBq (10 Ci) attached to a stainless steel cable. The source is driven by remote control between the storage safe located at the unit and user-programmed positions within the lumen of applicators implanted inside a patient. Treatment planning algorithms calculate the dose distribution in these implants using a formalism which includes several variables that describe the radiation properties of the HDR

Correspondence to: Matthew B. Podgorsak, Ph.D., Department of Radiation Medicine, Roswell Park Cancer Institute, Elm and Carlton Streets, Buffalo, NY, 14263.

UDC: 615.849.2:539.12.08

Ir-192 source.^{1,2} Currently, it is predominately low dose-rate (LDR) Ir-192 decay data that is used in HDR Ir-192 dosimetry calculations. Recent characterizations of the HDR Ir-192 source, however, have shown that some radiation parameters are highly source-type specific,^{3,4} suggesting that the use of LDR Ir-192 decay data in dosimetry calculations for HDR Ir-192 implants may be inappropriate.

One radiation parameter that has not yet been specifically determined for HDR Ir-192 sources is the air kerma-rate constant $(\Gamma_\delta)_K$. This quantity, in units of $\text{Gy m}^2 \text{s}^{-1} \text{Bq}^{-1}$, is defined by the photon spectrum emitted by a source and is related to the exposure rate constant $(\Gamma_\delta)_X$. Assuming a value 33.97 J/C for $(\bar{W}/e)_{\text{air}}$, it can be shown that the ratio of $(\Gamma_\delta)_K$ to $(\Gamma_\delta)_X$ is $6.58 \times 10^{-17} \text{ Gy R}^{-1} \text{ h s}^{-1} \text{ Ci Bq}^{-1}$. There have been many publications that have reported values of $(\Gamma_\delta)_X$ for Ir-192 sources ranging from 0.400 to 0.496 $\text{R m}^2 \text{Ci}^{-1} \text{h}^{-1}$ ($(\Gamma_\delta)_K = 26.3 \times 10^{-18}$ to $32.6 \times 10^{-18} \text{ Gy m}^2 \text{s}^{-1} \text{Bq}^{-1}$).⁵⁻⁷ Recently, Ninkovic and Raicevic⁸ reported a value of $30.0 \times 10^{-18} \text{ Gy m}^2 \text{s}^{-1} \text{Bq}^{-1}$ for the air kerma rate constant of an unfiltered low dose rate Ir-192 source. For an Ir-192 source encapsulated in 0.15 mm of platinum, they quoted a value of $27.8 \times 10^{-18} \text{ Gy m}^2 \text{s}^{-1} \text{Bq}^{-1}$, approximately 7% lower than for the unfiltered source.

The large variation in the air kerma rate constant for Ir-192 sources in different configurations clearly demonstrates a strong dependence of this quality on source design, particularly the type and thickness of encapsulation surrounding the active source material. Because the design of an HDR Ir-192 source is different from any other Ir-192 source, it is not apparent which of the previously reported values of $(\Gamma_\delta)_K$ should be used in HDR Ir-192 dosimetry calculations. A value of $30.66 \times 10^{-18} \text{ Gy m}^2 \text{s}^{-1} \text{Bq}^{-1}$ ($0.466 \text{ Rm}^2 \text{Ci}^{-1} \text{h}^{-1}$) has been adopted by manufacturers of the source and several brachytherapy treatment planning systems, while standardized calibration laboratories use a value of $30.24 \times 10^{-18} \text{ Gy m}^2 \text{s}^{-1} \text{Bq}^{-1}$ ($0.4596 \text{ Rm}^2 \text{Ci}^{-1} \text{h}^{-1}$). This latter value is calculated from a theoretical modeling of the HDR Ir-192 spec-

trum based on attenuation in the source encapsulation of known photons emitted from Ir-192. Although both these values are well within the range of those previously reported, they are significantly different from each other and, furthermore, the methodology used in their determination is not in all cases entirely clear. It is the purpose of this paper to describe a measurement of the HDR Ir-192 photon spectrum and a subsequent evaluation of the air kerma-rate constant for these sources.

Materials and methods

HDR Ir-192 source driven by the Microselectron

The activation of an HDR Ir-192 source requires approximately 6 weeks of irradiation by the typical thermal neutron fluxes in most reactors used to produce these sources.⁹ Prior to placement inside a reactor, the major component of the source material is expected to be Ir-191. The most likely activation therefore follows the Ir-191 (n, γ) Ir-192 reaction. Once activated to an activity of $\sim 370 \text{ GBq}$, the source is removed from the reactor and carefully encapsulated in a stainless steel capsule. Even though technically more difficult, encapsulation of the source must be done only after activation. This is because some components of stainless steel (mostly iron-58, chromium-50, and cobalt-59) have non-negligible neutron activation cross-sections and could themselves be activated by thermal neutrons and contaminate the HDR source photon spectrum.^{10,11} The source manufacturing process is completed by welding a stainless steel cable to the source capsule. The manufacturer (Mallinckrodt Diagnostica, Petten, Holland) then waits approximately one week before releasing the source for clinical use. This delay allows the Ir-194 contaminant, produced alongside Ir-192, to decay to the point where it will not contribute significantly to the energy spectrum of a clinical HDR Ir-192 source.

The most recent HDR Ir-192 source, shown

schematically in Figure 1,¹² was introduced in June 1991. In this design, the source capsule is 5.0 mm long with a diameter of 1.1 mm and a wall thickness of 0.25 mm. The active source material inside the capsule is 3.5 mm long and 0.6 mm in diameter. The center of source activity is 2 mm from the tip of the capsule.

Photon spectroscopy system: Description

Photon pulse-height spectra (PHS) were measured with a system consisting of a high-purity germanium (HPGe) detector (Canberra Industries, Inc., Meriden, CT) interfaced to a 4096 channel analyzer (MCA). The detector element was a coaxial germanium crystal (p-type) mounted in a cryostat consisting of a vacuum chamber thermally coupled to a liquid nitrogen heat sink. The impurity concentration in the germanium crystal was on the order of 10^{10} atoms/cm³. The crystal was held in place inside the cryostat by an aluminum holder 0.5 to 1.0 mm thick. The outer vacuum jacket was also made of aluminum, 1.5 mm thick on the sides and 0.5 mm thick at the entrance window. The HPGe crystal face was located 5 mm from the inside wall of the entrance window. A bias of 1000 V was applied to the crystal during acquisition of pulse height spectra.

Photon spectroscopy system: Detector calibration

Calibration of the spectroscopy system was done using standard Cobalt-60 (Co-60) and Europium-152 (Eu-152) sources (set no. 1718, Amersham International, Arlington Heights, IL). For acquisition of pulse-height spectra, the Eu-152 and Co-60 sources were positioned 50 cm from the front surface of the detector element (49.5 cm from the detector faceplate). The acquisition times were 4200 and 900 seconds, respectively. Any scattering surface was at least 1 m from both the source and detector crystal. A background spectrum was collected over a period of 1628 seconds, and was prorated

to either 4200 or 900 seconds. The number of counts $N(c)$ in the vicinity of each peak in the background-corrected Co-60 and Eu-152 pulse height spectra was then fitted with the following equation:

$$N(c) = a_1 + a_2 \exp \left[-\frac{(c - a_3)^2}{a_4^2} \right] + a_5(a_3 - c), \quad (1)$$

where c is channel number. Equation (1) includes terms for the following four components of the pulse-height spectrum in the vicinity of each peak: (1) a smoothly varying background signal produced by Compton interactions of higher energy photons in the detector crystal followed by escape of a scattered photon, (2) a Gaussian contribution from photoeffect interactions where the photon energy is entirely deposited in the detector with all resulting charge collected, (3) a low energy tail on the Gaussian distribution arising from imperfect charge collection in some regions of the detector or secondary electron or bremsstrahlung escape from the active volume, and (4) a step-like rise or fall in the Compton continuum due to Compton processes where the recoil electron receives almost all of the transferred energy.

Next, the parameters of Eq. (1) were used to derive two calibration models. The first was a second order polynomial in channel number relating the energy of a photon to the center of its Gaussian distribution. The correlation coefficient for the fit was 0.99999998, demonstrating an excellent fit. The second model, initially proposed by Singh,¹³ related the efficiency for a full-energy event to the energy of the photon interacting in the detector. The maximum deviation of the model-predicted efficiency and the experimental values used in its determination was 3.4%, although most deviations were <1%. The magnitude of these deviations is typical for a calibrated HPGe detector.¹³

Lower activity HDR Ir-192 source

To simplify the spectral measurements and increase the accuracy of the resulting spectrum, an Ir-192 source activated to as low an activity

as technically possible was obtained from the manufacturer (Mallinckrodt Diagnostica, Petten, Holland). The source was physically identical to the clinical HDR Ir-192 source shown in Figure 1, except its activity was much lower,

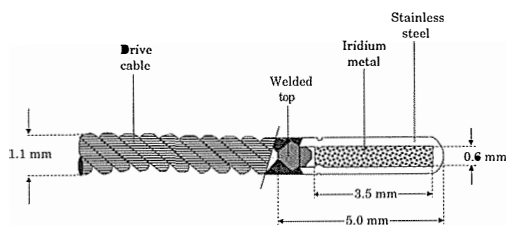


Figure 1. Schematic diagram showing a cross-section through the center of an HDR Ir-192 source remotely afterloaded by the Nucletron Microselectron. The diagram shows the most recent source design. The source is encapsulated in a 0.25 mm thick stainless steel capsule and a stainless steel cable connects the source capsule to the mechanical drivers inside the afterloader.

thus minimizing the effects of pulse pile-up and detector saturation on the measured pulse height spectrum. An initial calibration of the source was done with an HDR-1000 well ionization chamber (Standard Imaging, Middleton, WI), itself calibrated with a clinical HDR Ir-192 source whose air kerma strength had been determined using the inverse-square method.^{14,15} The signal to noise ratio for ionization current readings with this source was > 600 . The air kerma strength of the source was found to be $1.929 \times 10^{-6} \text{ Gy m}^2 \text{ h}^{-1}$. According to the HDR-1000 calibration certificate, the uncertainty in this value is $\pm 2\%$. In practice, though, the error is most likely very much less than 1%, and will be neglected in the remainder of this paper. A second calibration done approximately two weeks later and just before acquisition of the pulse height spectrum gave an air kerma strength of $1.692 \times 10^{-6} \text{ Gy m}^2 \text{ h}^{-1}$. Over the 14 day period of time between calibrations, the source decayed with a half-life of 73.833 days, in excellent agreement with the recently reported half-life for decay of clinical HDR Ir-192 sources.¹⁶

A schematic diagram of the set-up used for the measurement of the HDR Ir-192 pulse

height spectrum is shown in Figure 2. The source was suspended in air at a height of 120 cm above the ground at a distance of 130 cm from the front end of the detector element (129.5 cm from the detector faceplate). This extended source-detector distance was necessary to reduce the effects of pulse-pileup and detector saturation. The detector was placed at the end of a table at a height that centered the source on the detector faceplate. Only air was between the source and the detector faceplate. The operating parameters of the spectroscopy system were identical to those used for system calibration.

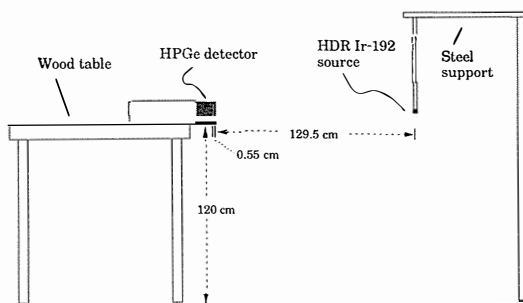


Figure 2. The experimental set-up for the measurement of the HDR Ir-192 pulse height spectrum. The walls in the room were all at least 100 cm either the detector or the source.

Results

HDR Ir-192 pulse height spectrum

The background corrected pulse-height spectrum for the lower activity HDR Ir-192 source is shown in Figure 3. The acquisition time was 1254 seconds. The spectrum is comprised of 16 peaks superimposed on a varying Compton background. Analysis of the spectrum consisted of fitting Eq. (1) to the number of counts in the vicinity of each peak (approximate peak center ± 38 channels). In the case of a doublet, where the events from one gamma ray could contribute to the distribution of a nearby peak created primarily by a different gamma ray, the sum of two such equations was fit to the pulse height spectrum in the vicinity of the two peaks comprising the doublet. In this work, the crite-

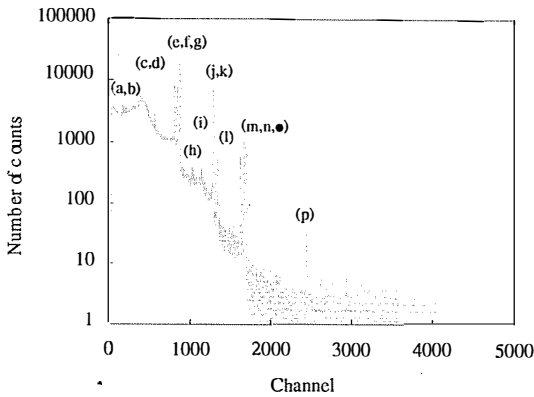


Figure 3. Background-corrected pulse height spectrum measured with an HDR Ir-192 source. The acquisition time was 1254 seconds.

tion for a doublet was the existence of two peaks within 30 channels of one another. Similarly, a triplet would be identified if there were three peaks within 60 channels. In the HDR Ir-192 pulse height spectrum shown in Figure 3, peaks (a) and (b), (c) and (d), (f) and (g), (k) and (l), and (n) and (o) were considered doublets; there were no triplets.

The position of each peak's center and the corresponding photon energy calculated from the calibration curve described above are listed in Table 1. The full-energy peak efficiency model derived with the calibration sources cannot be used directly with the Gaussian peak areas listed in Table 1. This is because the HDR Ir-192 pulse height spectrum was obtained with the source at a distance of 130 cm from the detector element, while the calibration curve was evaluated with pulse-height spectra measured at a source-detector distance of 50 cm. The measured peak area was corrected with a simple multiplicative correction factor based on geometrical considerations:

$$\text{area}(E) = a(E) \left[\frac{130}{50} \right]^2 \exp\{\mu(E)[130-50]\}, \quad (2)$$

where $\mu(E)$ is the linear attenuation coefficient in air (in cm^{-1}) for a photon of energy E ,¹⁷ $a(E)$ is the area of the Gaussian distribution corresponding to that photon in the measured pulse-height spectrum (source-detector distance = 130 cm), and $\text{area}(E)$ is the area that would

Table 1. Fitting and efficiency data for the HPGc detector used in this work. The numbers in brackets are the uncertainty in the value above each bracket.

Peak	Position of maximum (channel)	Photon energy E (keV)	Efficiency $\eta(E)$ ($\times 10^{-4}$)	area(E) (count* channel)
(a)	179.83 (0.12)	64.72 (0.05)	2.8000	118836.11 (3976.51)
(b)	206.33 (0.21)	74.29 (0.08)	2.8000	58822.17 (3567.71)
(c)	558.69 (1.73)	201.55 (0.62)	2.0035	13941.29 (4665.31)
(d)	570.37 (0.23)	205.77 (0.08)	1.9006	80685.99 (4143.62)
(e)	820.12 (0.02)	295.96 (0.01)	0.9767	549015.61 (3155.69)
(f)	854.75 (0.02)	308.46 (0.01)	0.9250	539980.08 (2888.58)
(g)	877.03 (0.01)	316.50 (0.01)	0.8951	1455272.55 (4305.75)
(h)	1037.25 (0.27)	374.35 (0.10)	0.7278	10258.73 (834.69)
(i)	1154.60 (0.42)	416.72 (0.15)	0.6376	8997.67 (1127.94)
(j)	1296.86 (0.01)	468.07 (0.01)	0.5502	531067.19 (1974.23)
(k)	1342.63 (0.06)	484.59 (0.02)	0.5260	34556.46 (669.86)
(l)	1355.55 (0.44)	489.25 (0.16)	0.5195	3662.26 (579.75)
(m)	1630.74 (0.04)	588.58 (0.01)	0.4066	38703.94 (466.05)
(n)	1674.67 (0.04)	604.43 (0.02)	0.3934	67144.46 (860.98)
(o)	1696.91 (0.06)	612.45 (0.02)	0.3855	42126.47 (813.53)
(p)	2450.51 (0.24)	884.30 (0.09)	0.2402	1723.80 (121.64)

have been measured were the source-detector distance equal to that in the calibration geometry (50 cm). The equivalence of energy calibration curves measured at different distances with identical detector operating characteristics has been demonstrated by Kamboj et al.¹⁸ They measured the full-energy peak efficiency for an HPGc detector with radium-226 (Ra-226) sources placed at distances of 53.5 and 164 cm from the detector, and they found identical calibration curves once inverse square fall-off photon fluence and photon attenuation in the air between the two measurement points were accounted for. Table 1 lists each identified photon in the HDR Ir-192 pulse-height spectrum along

with its efficiency for a full-energy interaction with the detector and the corrected area under the peak evaluated using Eq.(2).

Air kerma rate constant

The air kerma strength K_{air} of the HDR Ir-192 source at the beginning of the acquisition of the pulse height spectrum was $1.689 \times 10^{-6} \text{ Gy m}^2 \text{ h}^{-1}$ ($4.692 \times 10^{-10} \text{ Gy m}^2 \text{ s}^{-1}$) $\pm 2\%$. It can be shown that over the acquisition time of the HDR Ir-192 pulse height spectrum ($t = 1254$ seconds) the total air kerma was $5.883 \times 10^{-7} \text{ Gy m}^2 \pm 2\%$.

The emission frequency $f(E)$ of each identified photon of energy E in the HDR Ir-192 pulse height spectrum, given in units of number of photons emitted per parent decay, is given by:

$$f(E) = \frac{\text{area}(E)}{\eta(E)N}, \quad (3)$$

where $\text{area}(E)$ in the corrected area under each full energy peak, $\eta(E)$ is the full-energy peak efficiency, and N is the total number of decays of the parent atom. Calculating the number of HDR Ir-192 decays from the pulse height spectrum shown in Figure 3 is imprecise since the Compton continuum upon which the full-energy events are superimposed is not negligible, and the true detector crystal collecting volume is not known. It is, however, possible to relate N to the air kerma K_{air} as follows:

$$N = \frac{K_{\text{air}}}{(\Gamma_{\delta})_K}, \quad (4)$$

Substituting Eq. (4) into Eq. (3) gives

$$f(E) = \frac{\text{area}(E) \left[\frac{K_{\text{air}}}{(\Gamma_{\delta})_K} \right]^{-1}}{\eta(E)}. \quad (5)$$

Solving Eq. (5) for $(\Gamma_{\delta})_K$ results in the following equation for the air kerma rate constant:

$$(\Gamma_{\delta})_K = \frac{f(E) \eta(E) K_{\text{air}}}{\text{area}(E)}. \quad (6)$$

The necessary information to evaluate $(\Gamma_{\delta})_K$ using Eq. (6) for the HDR Ir-192 source has

either been determined in this work ($\eta(E)$, K_{air} , $\text{area}(E)$) or can be estimated from the literature ($f(E)$). The full energy peak efficiency $\eta(E)$ and the corrected area $\text{area}(E)$ are listed in Table 1. The uncertainty in the corrected areas listed in Table 1 vary greatly depending on the peak. Not surprisingly, the four lowest fractional uncertainties occur with the four most prominent peaks in the pulse-height spectrum. These uncertainties range from 0.3 to 0.6% for peaks representing the following energies: 295.96, 308.46, 316.50, and 468.07 keV. The uncertainties in the corrected area of the other peaks are all $> 2\%$, too high to suggest use of data from these peaks in Eq. (6).

To approximate $f(E)$ for a photon of energy E in the HDR Ir-192 photon spectrum, the emission frequencies for a bare Ir-192 source¹⁹ can be corrected for photon attenuation in the stainless steel encapsulation surrounding the HDR Ir-192 source. Assuming stainless steel to be equivalent to iron in attenuation characteristics and using attenuation coefficients found in the literature,¹⁷ the correction for attenuation in the encapsulation represents a 1.7% decrease in $f(E)$ for the 468.07 keV photon and a 2.1% decrease in $f(E)$ for the 295.96, 308.46, and 316.50 keV photons. The corrected emission frequencies to be used in Eq. (6) are therefore 0.277, 0.287, 0.813, and 0.469 for the following photons, respectively: 295.96, 308.46, 316.50, and 468.07 keV. Using Eq. (6) with pulse height spectrum data from each distribution corresponding to these four photons and the air kerma calculated above gives the following respective values of $(\Gamma_{\delta})_K$: $(29.02 \pm 0.53) \times 10^{-18}$, $(28.95 \pm 0.46) \times 10^{-18}$, $(29.41 \pm 0.20) \times 10^{-18}$, and $(28.62 \pm 0.53) \times 10^{-18} \text{ Gy m}^2 \text{ Bq}^{-1} \text{ s}^{-1}$. These values are all equal within experimental error. The average value is $(29.02 \pm 0.26) \times 10^{-18} \text{ Gy m}^2 \text{ Bq}^{-1} \text{ s}^{-1}$ ($0.441 \pm 0.004 \text{ R m}^2 \text{ Ci}^{-1} \text{ h}^{-1}$).

Discussion

Table 2 lists the energy and emission frequency of each photon component of the Ir-192 decay scheme described above alongside those of the

Table 2. HDR Ir-192 photon spectrum components compared to unencapsulated Ir-192 spectral

Peak	Photon energy (HDR Ir-192) (keV)	Photon energy (ref. [19]) (keV)	Emission frequency (HDR Ir-192) (γ 's/decay)	Emission frequency (ref. [19]) (γ 's/decay)
		7.822		0.00027
		8.266		0.00076
		8.904		0.0060
		9.337		0.000083
		9.435		0.0164
		9.975		0.000270
		10.469		0.0063
		11.174		0.0177
		12.213		0.00113
		13.025		0.00317
		61.485		0.0116
(a)	64.72 ± 0.05	63.000	0.021 ± 0.002	0.0200
		65.122		0.0266
		66.831		0.0456
		71.313		0.0069
(b)	74.29 ± 0.08	73.643	0.010 ± 0.001	0.00174
		75.634		0.0159
		78.123		0.00415
		136.34347		0.00181
		177.00		0.000073
(c)	201.55 ± 0.62	201.3805	0.003 ± 0.0005	0.00455
(d)	205.77 ± 0.08	205.79581	0.021 ± 0.001	0.0318
		219.221		0.000016
		283.2671		0.00252
(e)	295.96 ± 0.01	295.9582	0.277 ± 0.011	0.283
(f)	308.46 ± 0.01	308.45689	0.287 ± 0.012	0.293
(g)	316.50 ± 0.01	316.50789	0.801 ± 0.033	0.830
		329.348		0.00016
(h)	374.35 ± 0.10	374.5204	0.007 ± 0.001	0.00709
(i)	416.72 ± 0.15	416.4714	0.007 ± 0.001	0.00667
		420.601		0.00064
(j)	468.07 ± 0.01	468.07151	0.476 ± 0.021	0.477
(k)	484.59 ± 0.02	484.6473	0.032 ± 0.001	0.0313
		485.60		0.000022
(l)	489.25 ± 0.16	489.0626	0.003 ± 0.001	0.00432
(m)	588.58 ± 0.01	588.5845	0.047 ± 0.002	0.0447
		593.48		0.000438
(n)	604.43 ± 0.02	604.41463	0.084 ± 0.004	0.0823
(o)	612.45 ± 0.02	612.46561	0.054 ± 0.002	0.0534
		703.867		0.000058
(p)	884.30 ± 0.09	884.5418	0.004 ± 0.001	0.00284
		1061.55		0.000523
		1090.01		0.000011
		1378.05		0.000016

HDR Ir-192 spectrum determined in this work. The emission frequencies of the photons emitted by the HDR Ir-192 source were calculated using Eq. (5) with parameter values taken from Table 1. Figure 4 is a bar plot of the HDR Ir-192 photon spectrum compared with the pho-

ton spectra reported by several authors for unencapsulated Ir-192 sources.^{8,19,20} All photons, including γ -rays and characteristic x-rays, with emission frequencies greater than 0.003 (0.3%) were identified in the HDR Ir-192 pulse-height spectrum, with the following ex-

ceptions. First, Table 2 shows that the decay of Ir-192 produces several characteristic x-rays with energies between 7.822 and 13.025 keV. The HDR Ir-192 pulse height spectrum, however, shows no peaks below channel 180 (corresponding to an energy of ~ 63 keV) where one would expect Gaussian distributions for each of these photons. Complete absorption of photons with energies below ~ 60 keV in encapsulated Ir-192 sources has been suggested by Ninkovic and Raicevic,⁸ in evaluating the air kerma rate constant for an Ir-192 source encapsulated in 0.15 mm of platinum, they assumed a cutoff photon energy δ of 136.6 keV. Second, the four characteristic x-rays in the energy range of 61 to 67 keV emitted by Ir-192 could not be resolved in the HDR Ir-192 pulse-height spectrum with the current spectroscopy system. Instead, a single photon of energy roughly equal to the average of the four (64.72 keV) is suggested. Similarly, the two x-rays in the energy range of 71 to 76 keV are treated as one photon of energy equal to 74.29 keV.

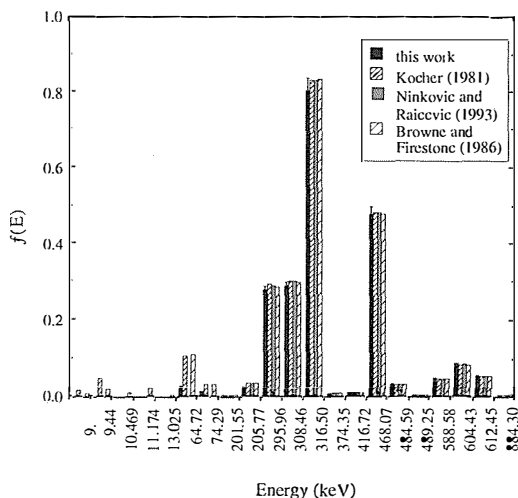


Figure 4. Photon spectrum for the HDR Ir-192 source evaluated in this work compared to the components of the photon spectra for bare Ir-192 sources with emission frequencies greater than 0.003. The energies listed are those determined in this work.

As shown in Table 2, the emission frequencies of high energy photons ($E > 500$ keV) emitted by the HDR Ir-192 source are essentially equal to those from a bare source. Lower

energy photons, however, have emission frequencies which are consistently lower than those emitted by a bare source. The magnitude of the difference increases with decreasing photon energy. A direct result of attenuation of lower energy photons in the stainless steel encapsulation is an increase in the average energy of the HDR Ir-192 photon spectrum. For the spectrum shown in Figure 4, the fluence-weighted and energy-fluence-weighted average energies are 371 and 402 keV, respectively. These are higher than the respective average energies calculated for the unencapsulated Ir-192 source spectrum (~ 346 and 395 keV) (20). Furthermore, the air kerma-rate constant calculated above is $\sim 5\%$ lower than the value currently used by the HDR Ir-192 source manufacturer and several brachytherapy planning systems to relate apparent source activity and reference air kerma rate. The apparent source activity is calculated from the measured reference air kerma rate and the air kerma rate constant only to facilitate understanding of the amount of radioactivity present in the source. Based on the apparent activity, a planning algorithm calculates the corresponding air kerma strength using an air kerma rate constant and then continues with the evaluation of the dose distribution. The clinical implications of a discrepancy in the air kerma rate constant now become clear. If the values of $(\Gamma_{\delta})_K$ used by a physicist (in calculating apparent activity from measured air kerma strength) and a planning system (doing the reverse calculation) are not the same, then the value of the source reference air kerma rate calculated by the treatment planning system will not equal the measured value. Inaccuracy in the calculated dose distribution with a subsequent dose delivery error will result directly from this discrepancy. The magnitude of the error will depend on the ratio of the two air kerma rate constants. The value of the air kerma rate constant has no effect on the dose distribution and subsequent dose delivery provided a consistent value is used throughout the source calibration and dose calculation procedures. As a result, the air kerma rate constant is a “dummy” constant in dose

calculation algorithms for sources calibrated in units of reference air kerma-rate.

The use of reference air kerma rate in place of activity for brachytherapy sources has been suggested several times in the recent literature.²¹⁻²³ Surprisingly, activity remains the dominant unit used for specification of HDR sources. In view of the potentially serious dose delivery errors resulting from the use of either air kerma rate or exposure rate constant in conjunction with source activity, we strongly encourage manufacturers of brachytherapy sources and treatment planning systems to eliminate activity as the measure of source strength and instead use reference air kerma rate. Since all HDR Ir-192 sources are calibrated in terms of reference air kerma rate, it makes little sense to use a quantity other than reference air kerma rate to describe the strength of these sources. While familiarity of the magnitude of the activity unit allows for a "feeling" of the amount of radioactivity present in a source, the radiation therapy community will eventually discover the same "feeling" from the magnitude of the reference air kerma-rate.

Conclusions

An estimate of the photon spectrum emitted by a clinical HDR Ir-192 source was made based on the pulse-height spectrum measured with a lower activity version of the source. The half-life for decay of this lower activity source was equal, within experimental error, to the value reported for clinical sources. This similar decay rate, coupled with the fact that the lower activity HDR Ir-192 source was manufactured to the same dimensional specifications as the clinical version, suggests that the low activity source had decay properties similar to a clinical source. Therefore, any radiation parameters evaluated from these properties will also pertain to clinical sources. Qualitatively, the photon spectrum showed that photons with an energy less than 60 keV do not escape the source capsule. Those most notably absent are the relatively abundant 9 and 9.44 keV photons

that are a result of the decay of Ir-192. Overall, all photons with energies below 500 keV are attenuated. The emission frequencies of higher energy photons, though, were identical to those from a bare Ir-192 source, suggesting negligible attenuation of these high energy photons in the stainless steel encapsulation.

A direct result of the difference in photon spectra is an increase in the fluence-weighted and energy-fluence-weighted average energies of the HDR Ir-192 source relative to the respective average energies of a pure Ir-192 source. Consequently, the air kerma rate constant evaluated from the measured HDR Ir-192 photon spectrum was ~5% lower than the value for a bare Ir-192 source. The air kerma rate constant was also lower than the value currently used by treatment planning systems. The serious potential clinical implications resulting from this discrepancy in air kerma rate (and exposure rate) constant strongly support the abolishment of source activity in favor of reference air kerma-rate for HDR Ir-192 source strength specification. This would make use of a modifying constant such as the air kerma rate or exposure rate constant unnecessary, and thus prevent dose delivery errors that could result from a misunderstanding of the value of either constant.

Acknowledgments

We are grateful to Dr. Edgar Loeffler of Nuclectron Corporation for commissioning the lower activity version of the HDR Ir-192 source used in this work. Also appreciated are numerous helpful discussions with Drs. Loeffler, Paul DeLuca, Jr., Rock Mackie, and Wayne Newhauser.

References

1. Killian H, Baier K, Loeffler E, Sussenbach K, Dorner K. A comparison of different planning algorithms used in interstitial radiotherapy with iridium-192 wires. In: Mould RF, ed., *Brachytherapy 2*. Holland: Nuclectron, Leersum: 1989: 92-100.
2. van der Laarse R. The Selectron treatment planning system. *Proceedings of the 7-th International Conference on the 7-th International Conference*

- on the use of Computers in Radiation Therapy. Japan: 1980.
3. Park HC, Almond PR. Evaluation of the buildup effect of an Ir-192 high dose-rate brachytherapy source. *Med Phys* 1992; **19**: 1293–7.
 4. Podgorsak MB. Radiation parameters of high dose rate iridium-192 sources. *Ph.D. thesis*, University of Wisconsin; 1993.
 5. Glasgow GP, Dillman LT. Specific gamma ray constant and exposure rate constant of Ir-192. *Med Phys* 1979; **6**: 49–52.
 6. Guiho JP, Hillion P. Table de quelque constantes de debit d'exposition. *Intern J Appl Rad Isotopes* 1974; **25**: 105–11.
 7. National Council on Radiation Protection and Measurements (NCRP). Report 41. *Specification of gamma-ray brachytherapy sources*. Washington: NCRP Publications, 1974.
 8. Ninkovic MM, Raicevic JJ. The air-kerma rate constant of Ir-192. *Health Phys* 1993; **64**: 79–81.
 9. Loeffler E. (personal communication); 1993.
 10. Das KR. Co-60 activity in Ir-192 seeds. *Health Phys* 1993; **64**: 183–6.
 11. Weast RC. *CRC Handbook of Chemistry and Physics*. 61st edition. CRC Press, Boca Raton, 1980: B–313.
 12. Mallinckrodt Diagnostica. HDR Ir-192 calibration certificate. Holland: Petten, 1993.
 13. Singh R. Validity of various semi-empirical formulae and analytical functions for the efficiency of Ge(Li) detectors. *Nucl Instr and Meth* 1976; **136**: 543–9.
 14. Goetsch SJ, Attix FH, Pearson DW, Thomadsen BR. Calibration of Ir-192 high-dose-rate afterloading systems. *Med Phys* 1991; **18**: 462–7.
 15. Goetsch SJ, Attix FH, DeWerd LA, Thomadsen BR. A new re-entrant ionization chamber for the calibration of Ir-192 high dose rate sources. *Int J Radiat Oncol Biol Phys* 1992; **24**: 167–70.
 16. Podgorsak MB, DeWerd LA, Paliwal BR. The half-life of high dose rate Ir-192 sources. *Med Phys* 1993; **20**: 1257–9.
 17. National Institute of Standards and Technology (NIST). Report NISTIR 4680. *Mass Energy-Transfer and Mass Energy-Absorption Coefficients, Including In-Flight Positron Annihilation for Photon Energies 1 keV to 100 MeV*. Gaithersburg: U.S. Department of Commerce, 1991.
 18. Kamboj S, Lovett D, Kahn B, Walker D. Radium needle used to calibrate germanium gamma-ray detector. *Health Phys* 1993; **64**: 300–5.
 19. Kocher DC. Radioactive Decay Tables, Report TIC-1102C. U.S. Department of Energy, 1981: 175–6.
 20. Browne E, Firestone RB. Table of Radioactive Isotopes. In: Shirley VS ed. New York: Wiley, 1986; 192–2.
 21. American Association of Physicists in Medicine (AAPM). Report 21. *Specification of brachytherapy source strength*. New York: American Institute of Physics, 1987.
 22. American Association of Physicists in Medicine (AAPM). Report 41. *Remote afterloading technology*. New York: American Institute of Physics, 1993.
 23. British Institute of Radiology (BIR). *Recommendations for brachytherapy dosimetry*. London: BIR publishing, 1993.